Article

Chemical Modification and Detoxification of the *Pseudomonas aeruginosa* Toxin 2-Heptyl-4-hydroxyquinoline *N*-oxide by Environmental and Pathogenic Bacteria

Sven Thierbach, Franziska S. Birmes, Matthias C Letzel, Ulrich Hennecke, and Susanne Fetzner

ACS Chem. Biol., **Just Accepted Manuscript** • DOI: 10.1021/acschembio.7b00345 • Publication Date (Web): 14 Jul 2017

Chemical Modification and Detoxification of the *Pseudomonas aeruginosa* Toxin 2-Heptyl-4-hydroxyquinoline *N*-oxide by Environmental and Pathogenic Bacteria

Sven Thierbach[†], Franziska S. Birmes[†], Matthias C. Letzel[‡], Ulrich Hennecke[‡], and Susanne Fetzner[†*]

[†]Institute for Molecular Microbiology and Biotechnology, University of Münster, 48149 Münster, Germany

[‡]Organic Chemistry Institute, University of Münster, 48149 Münster, Germany

Abstract

2-Heptyl-4-hydroxyquinoline *N*-oxide (HQNO), a major secondary metabolite and virulence factor produced by the opportunistic pathogen *Pseudomonas aeruginosa,* acts as potent inhibitor of respiratory electron transfer and thereby affects host cells as well as microorganisms. In this study, we demonstrate the previously unknown capability of environmental and pathogenic bacteria to transform and detoxify this compound. Strains of *Arthrobacter* and *Rhodococcus* spp. as well as *Staphylococcus aureus* introduced a hydroxyl group at C-3 of HQNO, whereas *Mycobacterium abscessus, M. fortuitum* and *M. smegmatis* performed an *O*-methylation, forming 2-heptyl-1-methoxy-4-oxoquinoline as initial metabolite. *Bacillus* spp. produced the glycosylated derivative 2-heptyl-1-(*β*-D-glucopyranosydyl)-4-oxoquinoline. Assaying the effects of these metabolites on cellular respiration and on quinol oxidase activity of membrane fractions revealed

that their EC_{50} values were up to two orders of magnitude higher than that of HQNO. Furthermore, cellular levels of reactive oxygen species were significantly lower in presence of the metabolites than under influence of HQNO. Therefore, the capacity to transform HQNO should lead to a competitive advantage against *P. aeruginosa.* Our findings contribute new insight into the metabolic diversity of bacteria, and add another layer of complexity to the metabolic interactions which likely contribute to shaping polymicrobial communities comprising *P. aeruginosa.*

Keywords:

Pseudomonas aeruginosa, Mycobacterium, Staphylococcus, Bacillus, antibiotic, respiration, alkylhydroxyquinoline *N*-oxide, *O*-methylation, glucosylation, hydroxylation, biotransformation, detoxification

INTRODUCTION

Pseudomonas aeruginosa is a ubiquitous Gram-negative γ-proteobacterium that inhabits soil and aqueous environments. As one of the most important opportunistic human pathogens, it can cause serious and life-threatening infections in immunocompromised and cystic fibrosis (CF) patients.[1] Many CF patients experience an age dependent colonization pattern, with *Staphylococcus aureus* being the prevalent pathogen in children and adolescents, which is replaced by *P. aeruginosa* in adults, however, the CF lung microbiome can be highly diverse.[2,3] CF-related lung disease also is a risk factor for chronic pulmonary infection with nontuberculous mycobacteria (NTM). NTM are detected with increasing prevalence in the CF population, with *Mycobacterium abscessus* being the most pathogenic and antibiotic-resistant species.[4-6]

P. aeruginosa produces an arsenal of virulence factors to colonize the host and to escape immune defenses.[1,7] Many of the extracellular factors, such as the redox-active pigment pyocyanin, rhamnolipid surfactants, siderophores, and secondary metabolites deriving from the 2-alkyl-4(1*H*)-quinolone biosynthetic pathway, not only affect the host but also have a negative impact on other bacteria. Especially the 2-alkyl-4(1*H*)-quinolones (AQs), which differ in the length and degree of saturation of the alkyl side chain, the substituent (–H or –OH) at the C3 position, and the oxidation state of the quinoline nitrogen, exert various and often multiple biological activities.[8-15]

2-Heptyl-4-hydroxyquinoline *N*-oxide (HQNO), one of the most abundant AQ compounds synthesized by *P. aeruginosa*, reaches concentrations ranging from few μM up to 35 μM in planktonic cultures[16-18] and has been found in sputum, plasma and urine from CF patients infected with *P. aeruginosa*.[19,20] HQNO binds to the quinone reduction (Q_i) site of the respiratory menaquinol/ubiquinol:cytochrome *c* oxidoreductase (the cytochrome bc_1 complex) and inhibits

respiratory electron transfer.[21] It also inhibits quinol oxidase activity of cytochrome bo_3 and *bd*, [22,23] and type II NADH-quinone oxidoreductase (NDH-2) involved in bacterial respiratory chains.[24] Auto-poisoning of the *P. aeruginosa* cytochrome bc_1 complex by HQNO induces a burst of reactive oxygen species (ROS) and affects membrane potential and permeability, finally causing autolysis.[25] Together with siderophores, HQNO is primarily responsible for *P. aeruginosa*-mediated killing of *S. aureus*.[26] Long-term exposure of *S. aureus* to HQNO moreover selects for small-colony variants (SCVs), which are well known for persistence in chronic infections.[20]

The complexity of polymicrobial infections in the CF lung raises the question of whether competitors have evolved strategies to inactivate the toxic secondary metabolites produced by *P. aeruginosa*. The same question applies to polymicrobial communities in environmental settings, such as soil habitats. From a soil sample, we previously isolated a *Rhodococcus erythropolis* strain with the ability to degrade the *P. aeruginosa* quorum sensing molecules 2-heptyl-4-hydroxyquinoline (HHQ) and 2-heptyl-3-hydroxy-4(1*H*)-quinolone (*Pseudomonas* quinolone signal, PQS) to anthranilic acid.[27] In this study, we tested a set of environmental and pathogenic bacteria for their ability to convert HQNO, identified the major metabolites formed from HQNO biotransformation, and assessed their effect on bacterial respiration, quinol oxidase activity, and induction of ROS formation.

RESULTS AND DISCUSSION

Three different ways for transforming HQNO. To investigate whether bacteria are capable of degrading the *P. aeruginosa* toxin HQNO, we used well-known model organisms (*Escherichia coli*, *Corynebacterium glutamicum, Bacillus* spp.), representatives of bacteria

commonly found in soil and water (*Rhodococcus erythropolis, Arthrobacter* spp., and members of environmental NTM), and selected opportunistic pathogens co-existing with *P. aeruginosa* in clinical settings, e.g., in the lung of CF patients (*S. aureus, M. abscessus*).

FIGURE 1.

Cell suspensions of *B. subtilis* and *B. licheniformis* slowly consumed HQNO, with concomitant transient accumulation of two metabolites (Figure 1a). MS analysis of the first compound revealed an *m/z* of 422.217 ($[C_{22}H_{31}NO_7 + H^+]$), suggesting a hexosyl-HQNO (Table 1 and Supporting Figure S1a). When the growth medium was additionally supplemented with glucose or galactose, the first step of HQNO conversion was accelerated, and hexosyl-HQNO accumulated in significantly higher amounts (data not shown). The metabolite was extracted from galactose supplemented cultures of *B. subtilis* and purified by preparative HPLC for NMR analysis. Based on ^3J-coupling constants ^3J(H1''-H2'') = 8.3 Hz, ^3J(H2''-H3'') = 9.0 Hz, ^3J(H3''-H4'') = 9.3 Hz and ^3J(H4''-H5'') = 9.3 Hz indicating an all-*trans* substitution pattern, the sugar moiety was identified as glucose. The β-configuration was deduced from the ^3J(H1''-H2'') = 8.3 Hz coupling constant and the strong NOE between the H1'' and H5'' proton indicating a 1,3-diaxial relationship. The regiochemistry of the substitution was deduced from the strong NOE between the H8 proton of the quinoline system and the H1'' proton of the sugar unit. From these data, the metabolite was identified as 1-(*β*-glucopyranosydyl)-2-heptyl-4-hydroxyquinoline (G-HQNO; Table 1 and Supporting Figure S4).

The *m/z* of 522.233 ($[C_{26}H_{35}NO_{10} + H^+]$), observed for the second metabolite formed by the *Bacillus* strains tested, is consistent with an acylated – possibly succinylated – derivative of

glucosyl-HQNO (SG-HQNO) (Supporting Figure S1b). Treatment of this biotransformation intermediate with aqueous ammonia resulted in a deacylated but still glucosylated product with HPLC elution behavior and molecular mass identical to that of the first intermediate (*m/z* of 422.217), indicating acylation of the glucosyl residue instead of a substituent of the aromatic ring. MS/MS fragmentation of G-HQNO and SG-HQNO led to the same *m/z* of 260.166 with almost 100 % abundance (Supporting Figures S1c and S1d). When the metabolites were treated with zinc/acetic acid to reduce any residual N-O bond, the same product was formed from both compounds, which based on its HPLC retention time and UV spectrum was identified as HHQ. This supports the hypothesis that HQNO modification by the two *Bacillus* spp. takes place at the *N*-oxide and involves *O*-glucosylation and further acylation of the glucosyl residue. Other metabolites besides G- and SG-HQNO were not detected in extracts of *Bacillus* cultures. Either, further degradation proceeds without accumulation of intermediates, or intermediates formed escape extraction and/or UV detection.

Glycosylation and succinylation of natural products seem to be common strategies of bacilli. *B. subtilis* natto as well as *B. licheniformis* have been reported to produce succinylated isoflavone glycosides from soybean isoflavones.[28] Furthermore, the UDP-glycosyltransferase YjiC (from *B. licheniformis*) has been shown to glycosylate plant flavonoids, antibiotics such as mupirocin, and macrolides such as epothilone A.[29-32]

The three mycobacteria tested, *M. abscessus*, *M. fortuitum* and *M. smegmatis*, used another strategy to modify HQNO. All three species were found to form 2-heptyl-1-methoxy-4-oxoquinoline (HMOQ) as a major transient metabolite (Figure 1b and Table 1). The identity of HMOQ was established by comparison of its HPLC retention time and MS/MS fragmentation pattern with an authentic standard obtained by chemical synthesis (Supporting Figure S2). HPLC

analysis of samples taken after HMOQ had reached the peak concentration suggested formation of a multitude of metabolites at low concentrations which show UV spectra resembling that of HMOQ. Therefore, we tentatively assume that the compounds are structurally closely related, with modifications possibly introduced mainly to the alkyl chain.

Already decades ago, mycobacteria were observed to modify phenolic and catecholic compounds by methylation. *M. fortuitum* CG-2, an isolate from soil, is capable of *O*-methylating a plethora of chlorinated phenols, guaiacols, syringols, and hydroquinones, with a preference for *ortho*-chlorinated substrates.[33] *M. vanbaalenii* PYR-1 neutralizes the toxic effect of catechols by *O*-methylation[34], generating less reactive intermediates which in contrast to catechol do not promote formation of hydroxyl radicals by the Fenton reaction.[35]

Cell suspensions of *Arthrobacter* sp. Rue61a, *Paenarthrobacter aurescens* TC1, *R. erythropolis* BG43, *R. erythropolis* PR4, *S. aureus* Newman, and *S. aureus* USA-300 were also capable of converting HQNO (Figure 1c). MS analysis of the transiently accumulating metabolite revealed an *m/z* of 276.159 (for $[C_{16}H_{21}NO_3 + H^+]$), consistent with a hydroxylated form of HQNO (Table 1 and Supporting Figures S3a,b). The MS/MS fragmentation pattern as well as the ^{1}H-NMR data suggest the hydroxyl group to be located at the C3-position of the heteroaromatic ring (Supporting Figures S3c, S6). This is supported by the observation that zinc/acetic acid reduction of the *N*-oxide group of this compound yielded PQS, which was identified by HPLC and its characteristic UV spectrum. Hence, we propose that these Gram-positive bacteria hydroxylate HQNO to 2-heptyl-3,4-dihydroxyquinoline-*N*-oxide ("PQS-*N*-oxide", PQS-NO). The observed gradual decrease in PQS-NO levels in the *S. aureus* cultures (Figure 1c) may in parts be due to its spontaneous decomposition to PQS (half-life in sterile LB at 30 °C is 2.5 hours).

Formation of G- and SG-HQNO, HMOQ, and PQS-NO was organism-specific under the conditions of the biotransformation experiments. We did not detect G-HQNO or SG-HQNO in cultures other than *Bacillus* spp., or HMOQ in cultures other than *Mycobacterium* spp., and we also could not detect PQS-NO in *Bacillus* or *Mycobacterium* cultures.

For *C. glutamicum*, *E. coli* BL21, and *P. putida* KT2440, we could not observe any HQNO conversion under the conditions tested. The strains were still able to grow in presence of 10 µM HQNO.

Inhibitory effects of HQNO and its metabolites on cellular respiration and menaquinol oxidase activity. The antimicrobial activity of HQNO has been reported to be mainly due to inhibition of respiratory electron transfer. To find out whether the chemical modifications of HQNO performed by the bacteria tested correlate with detoxification, we compared the respiration activity of cell suspensions, as well as menaquinol oxidase activity of membrane preparations, in response to HQNO and to the major metabolite formed by the respective strain.

FIGURE 2.

Respiration of *B. subtilis* 168 cells was highly sensitive to HQNO which showed an EC_{50} value of 0.4 µM. Correspondingly, growth of freshly inoculated cultures was inhibited by 10 µM HQNO (Supporting Figure S7a). The menaquinol oxidase activity of membrane fractions prepared from *B. subtilis* was drastically inhibited by HQNO, with the EC_{50} value of 1.6 µM being slightly higher than that observed for cellular respiration (Figure 2a,d). In contrast, the EC_{50} of G-HQNO

on cellular respiration was more than two orders of magnitude higher, with a value of 84.4 μM being far above the range of physiological concentrations (Figure 2a). In line with the *in vivo* data, the menaquinol oxidase activity of membrane fractions was only weakly inhibited by G-HQNO, which under the conditions of the assay had an EC_{50} value of 128.4 μM (Figure 2d). Conjugation of HQNO with the bulky and polar glucose residue may efficiently prevent binding to the quinone/quinol binding sites of menaquinol oxidases. Additional acylation – possibly a succinylation – of G-HQNO by *Bacillus* could introduce a negative charge, which should support release of the compound from the membrane.

Cells of *M. abscessus* DSM 44196 as well as *M. smegmatis* mc^2 155 (data not shown) showed only little response to both HQNO and the metabolite HMOQ. At 100 μM of HQNO or HMOQ, the residual relative respiratory activities *of M. abscessus* were still 81% and 94%, respectively (Figure 2b). On the one hand, the complex cell wall of mycobacteria may protect them against toxic compounds. On the other hand, in order to maintain ATP levels the mycobacteria might reroute electron transfer by rapidly switching between terminal oxidases, thereby increasing O_2 consumption, as shown recently for *M. tuberculosis*.[36] In line with the insensitivity of respiratory activity of *M. abscessus* cells to HQNO, the growth curve of *M. abscessus* was unaffected by 10 μM HQNO (Supporting Figure S7b). However, *in vitro* experiments using membrane fractions of *M. abscessus* revealed significant inhibition of menaquinol oxidase activity by HQNO, with an EC_{50} value of 4 μM (Figure 2e), but much less sensitivity toward HMOQ. The estimated EC_{50} value for HMOQ of 189 μM suggests that methylation of the *N*-oxide is a highly efficient way to counteract poisoning of menaquinol oxidases.

S. aureus is well known to be very sensitive to HQNO.[20,26,37,38] This is reflected by inhibition of growth in presence of 10 μM HQNO, however, the cells resumed growth after having decreased

the HQNO levels by biotransformation (Supporting Figure S7c). For *S. aureus,* the EC_{50} value of HQNO on cellular respiration was determined as 3.2 μM. The hydroxylated metabolite, PQS-NO, showed only a slightly reduced inhibitory effect with an EC_{50} value of 12.3 μM (Figure 2c). The results of the menaquinol oxidase assays were similar, with HQNO acting as highly efficient inhibitor and PQS-NO also exerting a substantial inhibitory effect (Figure 2f), with estimated EC_{50} values for HQNO and PQS-NO of 0.2 μM and 1.8 μM, respectively.

Whereas HQNO hydroxylation to PQS-NO led to only moderate detoxification for *S. aureus*, the metabolites formed by *M. abscessus* and *B. subtilis* had EC_{50} values which were increased by more than one order of magnitude compared to that of HQNO. Therefore, modifying the *N*-oxide functional group appears to be an efficient strategy to detoxify HQNO as respiratory inhibitor.

Cellular ROS levels in presence of HQNO and its metabolites. Inhibition of quinone reduction at the Q_i site of the cytochrome bc_1 complex, using, e.g., antimycin A, has been reported to significantly increase ROS production at the Q_0 site.[39] To test for cellular ROS, we measured fluorescence intensities of 2′,7′-dichlorodihydrofluorescein (DCF), a fluorescent probe for cellular oxidant stress.[40]

FIGURE 3.

When cell suspensions were incubated with HQNO, a 2-fold and even 4-fold increase of DCF fluorescence was observed for *B. subtilis* 168 and *M. abscessus*, respectively, indicating elevated oxidative stress (Figure 3). Even though the presence of 100 μM G-HQNO or HMOQ, which still

showed some inhibition in the quinol oxidase assay, resulted in slightly higher DCF fluorescence increases compared to the DMSO controls, the ROS-inducing effect of the metabolites was significantly lower than that of HQNO.

Mycobacterial growth under aerobic conditions mainly relies on the cytochrome bc_1-aa_3 branch.[41] Thus, HQNO inhibition of cytochrome bc_1, which was reported to mediate ROS production when inhibited at the Q_i site[39], may account for the observed strong induction of ROS formation in *M. abscessus*. In contrast, *B. subtilis* uses a branched respiratory chain with cytochrome aa_3 and *bd* as terminal quinol oxidases, with cytochrome aa_3 as the major terminal oxidase during exponential growth.[42] Homologs of these quinol oxidases from other organisms as well as cytochrome aa_3 (Qox) of *B. subtilis* have been shown to be sensitive towards HQNO, but it has not been reported whether inhibition leads to ROS formation.[22,43,44] However, since electrons from the menaquinol pool of *B. subtilis* can also enter the cytochrome oxidase branch via the cytochrome *bc* complex[42], the observed moderate increase in ROS production in HQNO-treated cells of *B. subtilis* might be due to inhibition of cytochrome *bc*.

Surprisingly, *S. aureus* Newman did not show an altered DCF fluorescence increase in the presence of HQNO compared to the control (Figure 3). This may be due to the fact that *S. aureus* in contrast to the other model organisms tested completely lacks the bc_1 complex, and only possesses aa_3- and *bd*-type terminal oxidases.[45,46] Remarkably, PQS-NO even reduced the DCF fluorescence increase to almost 0.4-fold of the control, suggesting antioxidant capacity of this metabolite.

Conclusions. In this study, we demonstrate that bacteria have the capability to transform the respiratory inhibitor HQNO, a major toxin produced by the opportunistic pathogen *P.*

aeruginosa. Among the bacteria tested, we identified three different ways to covalently modify and detoxify the respiratory inhibitor HQNO, illustrated in Figure 4. *Bacillus* spp. initially transformed HQNO to the glucosylated derivative G-HQNO, which was significantly less inhibitory on respiration and menaquinol oxidase activity than HQNO, and induced less oxidative stress. The three *Mycobacterium* spp. tested catalyzed an initial *O*-methylation of the *N*-oxide, which also resulted in a substantial quenching of the inhibitory activity on quinol oxidase. Oxidative stress in mycobacteria was drastically increased by HQNO, whereas HMOQ showed an almost negligible effect. *S. aureus* as well as *Arthrobacter* and *Rhodococcus* spp. were found to introduce a hydroxyl substituent at C3 of HQNO, instead of modifying the *N*-oxide group. The resulting PQS-NO exhibited only slightly less respiratory inhibition than HQNO, but it quenched oxidative stress in *S. aureus*. The molecular mechanisms underlying the observed physiological effects of HQNO modification remain to be elucidated. However, our discovery of HQNO biotransformation and detoxification adds another layer of complexity to the multifaceted interactions within microbial communities. Microorganisms capable of detoxifying HQNO clearly should gain a competitive advantage in mixed-species microbial communities with *P. aeruginosa*. Thus, future studies should evaluate the significance of HQNO modification and degradation in the context of co-culture and co-infection. HQNO does not function as a quorum sensing signal molecule,[47] and the HQNO derivatives seem not to affect biofilm formation or to interfere with *P. aeruginosa* quorum sensing, as suggested by absence of effects on PQS and pyocyanin production (Supporting Figure S8). However, auto-poisoning of *P. aeruginosa* might be decreased in co-cultures,[25] and the HQNO metabolites might exert other biological activities. Thus, another key question is whether the metabolites influence interspecies behavior by affecting the phenotypes not only of *P. aeruginosa*, but also of other bacteria, fungi, and host cells. From a more pharmacological point of view, the selective chemical modification of the

heterocyclic *N*-oxide may also open up perspectives for the development of new bioactive compounds.

METHODS

Chemicals and chemical synthesis. Chemicals were purchased from Aldrich, Acros, TCI, or Merck, and used as received. HHQ and HQNO were prepared according to literature procedures.[48,49] A detailed description of the synthesis of 2-heptyl-1-methoxy-4-oxoquinoline (HMOQ) is provided in the Supporting Information.

***N*-oxide reduction.** HQNO metabolites were dissolved in 100% acetic acid and a few grains of zinc powder were added to reduce hydroxyquinoline *N*-oxides to the corresponding hydroxyquinolines. After incubation for 15 min at room temperature the suspension was centrifuged to pellet undissolved particles. The supernatant was dried to completion and the residual sample was redissolved in methanol for HPLC analysis.

Analytical methods. Detailed information about analytical and preparative HPLC, MS analyses and NMR analyses is given in the Supporting Information.

Bacterial strains and growth conditions. *R. erythropolis* BG43 (DSM 46869), *R. erythropolis* PR4 (NBRC 100887), *Arthrobacter* sp. Rue 61a (DSM 24942), *Paenarthrobacter* (formerly: *Arthrobacter*) *aurescens* TC1 (ATCC BAA-1386), *Corynebacterium glutamicum* (DSM 20300), *Bacillus subtilis* 168 (DSM 402), *Bacillus licheniformis* (DSM 13), *Pseudomonas putida* KT2440 (DSM 6125), *Staphylococcus aureus* Newman (NCTC 8178), *S. aureus* USA300[50] and *Escherichia coli* BL21 were grown in LB (lysogeny broth; 5 g/L yeast extract, 10 g/L peptone, tryptic digested, 10 g/L NaCl, pH 7.3) at 37°C (*E. coli*, *B. subtilis*, *S. aureus*) or 30°C (all other strains). *Mycobacterium abscessus* (DSM 44196), *M. fortuitum* (DSM 46621) and *M. smegmatis*

strain mc^2 155 (ATCC 700084) were cultivated at 37 °C in DSM 219 medium (per L: yeast extract 2.0 g; proteose peptone 2.0 g, casein peptone, tryptic digested, 2.0 g, $Na_2HPO_4 \times 12\ H_2O$ 2.5 g, KH_2PO_4 1.0 g, Na-citrate 1.5 g, $MgSO_4 \times 7\ H_2O$ 0.6 g, glycerol 50.0 ml, Tween 0.5 g, pH 7.0).

Biotransformation of HQNO and organic extraction. For biotransformation experiments, cells were pelleted by centrifugation (7,000 × *g*, 5 min) and resuspended in fresh medium adjusting an optical density (OD_{600nm}) of 2. HQNO (Enzo Life Sciences, dissolved in methanol) was added to each culture to a final concentration of 10 µM, and cultures were incubated under vigorous shaking at 37°C. At appropriate time intervals 1 mL samples were withdrawn and extracted three times with 0.5 mL ethyl acetate (acidified with 1 mL/L acetic acid) as described previously.[27] The organic phase was dried to completion and 200 µL methanol was added to redissolve the sample for HPLC analysis. For the preparation of larger amounts of the metabolites by biotransformation and preparative HPLC, cultures were fed with the synthesized HQNO.

Cellular respiration and quinol oxidase assay. To determine the effect of HQNO and HQNO metabolites on cellular respiration, exponentially growing cells were adjusted to an OD_{600} of 0.5. 1 mL cell suspension was mixed with 5 µL of the compound to be tested (dissolved in DMSO) and shaken vigorously for 10 min at room temperature prior to monitoring cellular O_2 consumption. The protocol used for preparation of cell membranes is provided in the Supporting Information. Inhibition of quinol oxidase activity of membrane fractions was measured using a coupled enzyme assay. The reaction was carried out in air-saturated 50 mM potassium phosphate buffer, pH 6.5, at room temperature. The quinol substrate 2,3-dimethyl-1,4-naphthoquinol ($DMNH_2$) was formed from 2,3-dimethyl-1,4-naphtoquinone (DMN, purchased from RareChemicals, Kiel, Germany) and NADH by DT-diaphorase (Sigma). The reaction mixture

(final volume of 500 µL) contained 250 µM DMN, 20 µg/mL DT-diaphorase, varying concentrations of HQNO or its metabolites, and 10-40 µL of the membrane fraction. The assay was started by the addition of 400 µM NADH. Autoxidation of reduced DMN was measured separately in the absence of the membrane fraction. For measuring cellular respiration as well as for the quinol oxidase assay, oxygen consumption was monitored with a Clark-type oxygen electrode equipped with a magnetically stirred chamber. Reference samples without inhibitors contained the same amount of DMSO. EC_{50} values were estimated from fitting the data to a dose response curve (Hill equation).

Cellular ROS detection. The cellular production of ROS in the presence of HQNO or its metabolites was measured using the cell permeable dye 2',7'-dichlorodihydrofluorescein diacetate (H_2DCF-DA, purchased from Sigma).[40] *B. subtilis*, *M. abscessus* and *S. aureus* were grown as described above. Cells were pelleted by centrifugation, resuspended in fresh medium adjusting an OD_{600} of 1, supplemented with 50 µM of H_2DCF-DA, and shaken vigorously at 37 °C for 30 min. Prior to the addition of 100 µM of HQNO or its metabolite, cells were washed once with phosphate buffered saline (PBS, pH 7.5) to remove residual extracellular dye, and resuspended in PBS. Suspensions of mycobacteria were additionally supplemented with 0.05% (w/v) Tween80. Aliquots of the cell suspensions were transferred to a 96-well microtiter plate (200 µL per well) and the fluorescence increase (Ex/Em of 490/510-570 nm) over 30 min was measured using the GloMax®-Multi+ microtiter plate reader (Promega). Results represent the mean of three independent experiments, each measured in three technical replicates.

AUTHOR INFORMATION

Corresponding Author

*E-mail: fetzner@uni-muenster.de. Tel. 049 (251) 8339824. Fax +49 (251) 8338388.

Author contributions

S.F. conceived the study. S.F. and S.T. coordinated the study. F.S.B. performed biotransformations and biofilm and pyocyanin assays. S.T. performed all other physiological and biochemical experiments. U.H. performed all chemical syntheses, NMR analyses, and together with M.C.L. performed MS analyses. All authors contributed to interpretation of data. S.F. and S.T. wrote the manuscript. S.T. and U.H. prepared the figures. All authors contributed to and approved the final version of the manuscript.

ACKNOWLEDGEMENTS

Research reported in this publication was supported by the Deutsche Forschungsgemeinschaft (grant FE 383/25-1 to S.F., and Heisenberg grant HE 6020/3-1 to U.H.). F.B. thanks the Studienstiftung des Deutschen Volkes for a PhD scholarship and support. We thank T. Martins and P. Fricke for help with biotransformation experiments and respiratory measurements, B. Kahl for providing *S. aureus* strains, and B. Philipp for access to the electrospray ionization ion trap mass spectrometer (DFG grant INST 211/646-1) which was used for initial MS analyses.

ASSOCIATED CONTENT

Supporting Information

Description of chemical syntheses, analytical procedures, membrane preparation protocols, and biofilm and pyocyanin assays; Figures S1-S6 providing supporting MS and NMR data; Figure S7 providing supporting information on the effect of HQNO on bacterial growth; Figure S8 providing supporting data on the effect of HQNO metabolites on *P. aeruginosa* (PDF file).

REFERENCES

(1) Lyczak, J. B., Cannon, C. L., and Pier, G. B. (2000) Establishment of *Pseudomonas aeruginosa* infection: lessons from a versatile opportunist. *Microbes Infect. 2*, 1051−1060.

(2) McGuigan, L., and Callaghan, M. (2015) The evolving dynamics of the microbial community in the cystic fibrosis lung. *Environ. Microbiol. 17*, 16−28.

(3) Palmer, G. C., and Whiteley, M. (2015) Metabolism and pathogenicity of *Pseudomonas aeruginosa* infections in the lungs of individuals with cystic fibrosis. *Microbiol. Spectr. 3*, MBP-0003-2014.

(4) Bar-On, O., Mussaffi, H., Mei-Zahav, M., Prais, D., Steuer, G., Stafler, P., Hananya, S., and Blau, H. (2015) Increasing nontuberculous mycobacteria infection in cystic fibrosis. *J. Cyst. Fibros. 14*, 53−62.

(5) Bryant, J. M., Grogono, D. M., Rodriguez-Rincon, D., Everall, I., Brown, K. P., Moreno, P., Verma, D., Hill, E., Drijkoningen, J., Gilligan, P., Esther, C. R., Noone, P. G., Giddings, O., Bell, S. C., Thomson, R., Wainwright, C. E., Coulter, C., Pandey, S., Wood, M. E., Stockwell, R. E., Ramsay, K. A., Sherrard, L. J., Kidd, T. J., Jabbour, N., Johnson, G. R., Knibbs, L. D., Morawska, L., Sly, P. D., Jones, A., Bilton, D., Laurenson, I., Ruddy, M., Bourke, S., Bowler, I. C., Chapman, S. J., Clayton, A., Cullen, M., Dempsey, O., Denton, M., Desai, M., Drew, R. J., Edenborough, F., Evans, J., Folb, J., Daniels, T., Humphrey, H., Isalska, B., Jensen-Fangel, S., Jönsson, B., Jones, A. M., Katzenstein, T. L., Lillebaek, T., MacGregor, G., Mayell, S., Millar, M., Modha, D., Nash, E. F., O'Brien, C., O'Brien, D., Ohri, C., Pao, C. S., Peckham, D., Perrin, F., Perry, A., Pressler, T., Prtak, L., Qvist, T., Robb, A., Rodgers, H., Schaffer, K., Shafi, N., van Ingen, J., Walshaw, M., Watson, D., West, N., Whitehouse, J., Haworth, C. S., Harris, S. R.,

Ordway, D., Parkhill, J., and Floto, R. A. (2016) Emergence and spread of a human-transmissible multidrug-resistant nontuberculous mycobacterium. *Science 354*, 751–757.

(6) Parkins, M. D., and Floto, R. A. (2015) Emerging bacterial pathogens and changing concepts of bacterial pathogenesis in cystic fibrosis. *J. Cyst. Fibros. 14*, 293−304.

(7) Gellatly, S. L., and Hancock, R. E. W. (2013) *Pseudomonas aeruginosa*: new insights into pathogenesis and host defenses. *Pathog. Dis. 67*, 159−173.

(8) Bredenbruch, F., Geffers, R., Nimtz, M., Buer, J., and Häussler, S. (2006) The *Pseudomonas aeruginosa* quinolone signal (PQS) has an iron-chelating activity. *Environ. Microbiol. 8*, 1318−1329.

(9) Diggle, S. P., Matthijs, S., Wright, V. J., Fletcher, M. P., Chhabra, S. R., Lamont, I. L., Kong, X., Hider, R. C., Cornelis, P., Cámara, M., and Williams, P. (2007) The *Pseudomonas aeruginosa* 4-quinolone signal molecules HHQ and PQS play multifunctional roles in quorum sensing and iron entrapment. *Chem. Biol. 14*, 87–96.

(10) Häussler, S., and Becker, T. (2008) The *Pseudomonas* quinolone signal (PQS) balances life and death in P*seudomonas aeruginosa* populations. *PLoS Pathog. 4*, e1000166.

(11) Mashburn, L. M., and Whiteley, M. (2005) Membrane vesicles traffic signals and facilitate group activities in a prokaryote. *Nature 437*, 422–425.

(12) Nguyen, A. T., Jones, J. W., Cámara, M., Williams, P., Kane, M. A., and Oglesby-Sherrouse, A. G. (2016) Cystic fibrosis isolates of *Pseudomonas aeruginosa* retain iron-regulated antimicrobial activity against *Staphylococcus aureus* through the action of multiple alkylquinolones. *Front. Microbiol. 7*, 1171.

(13) Park, S. Y., Heo, Y. J., Choi, Y. S., Déziel, E., and Cho, Y. H. (2005) Conserved virulence factors of *Pseudomonas aeruginosa* are required for killing *Bacillus subtilis*. *J. Microbiol. 43*, 443−450.

(14) Reen, F. J., Mooij, M. J., Holcombe, L. J., McSweeney, C. M., McGlacken, G. P., Morrissey, J. P., and O'Gara, F. (2011) The *Pseudomonas* quinolone signal (PQS), and its precursor HHQ, modulate interspecies and interkingdom behavior. *FEMS Microbiol. Ecol. 77*, 413−428.

(15) Toyofuku, M., Nakajima-Kambe, T., Uchiyama, H., and Nomura, N. (2010) The effect of a cell-to-cell communication molecule, *Pseudomonas* quinolone signal (PQS), produced by *P. aeruginosa* on other bacterial species. *Microbes Environ. 25*, 1−7.

(16) Lépine, F., Deziel, E., Milot, S., and Rahme, L. G. (2003). A stable isotope dilution assay for the quantification of the *Pseudomonas* quinolone signal in *Pseudomonas aeruginosa* cultures. *Biochim. Biophys. Acta 1622*, 36−41.

(17) Lépine, F., Milot, S., Déziel, E., He, J., and Rahme, L. G. (2004) Electrospray/mass spectrometric identification and analysis of 4-hydroxy-2-alkylquinolines (HAQs) produced by *Pseudomonas aeruginosa*. *J. Am. Soc. Mass Spectrom. 15*, 862−869.

(18) Ortori, C. A., Dubern, J. F., Chhabra, S. R., Cámara, M., Hardie, K., Williams, P., and Barrett, D. A. (2011) Simultaneous quantitative profiling of *N*-acyl-L-homoserine lactone and 2-alkyl-4(1*H*)-quinolone families of quorum-sensing signaling molecules using LC-MS/MS. *Anal. Bioanal. Chem. 399*, 839−850.

(19) Barr, H. L., Halliday, N., Cámara, M., Barrett, D. A., Williams, P., Forrester, D. L., Simms, R., Smyth, A. R., Honeybourne, D., Whitehouse, J. L., Nash, E. F., Dewar, J., Clayton, A., Knox, A. J., and Fogarty, A. W. (2015) *Pseudomonas aeruginosa* quorum sensing molecules correlate with clinical status in cystic fibrosis. *Eur. Respir. J. 46*, 1046−1054.

(20) Hoffman, L. R., Déziel, E., D'Argenio, D. A., Lépine, F., Emerson, J., McNamara, S., Gibson, R. L., Ramsey, B. W., and Miller, S. I. (2006) Selection for *Staphylococcus aureus* small-colony variants due to growth in the presence of *Pseudomonas aeruginosa*. *Proc. Natl. Acad. Sci. USA 103*, 19890–19895.

(21) Cooley, J. W., Ohnishi, T., and Daldal, F. (2005) Binding dynamics at the quinone reduction (Q_i) site influence the equilibrium interactions of the iron sulfur protein and hydroquinone oxidation (Q_o) site of the cytochrome bc_1 complex. *Biochemistry 44*, 10520−10532.

(22) Yap, L. L., Lin, M. T., Ouyang, H., Samoilova, R. I., Dikanov, S. A., and Gennis, R. B. (2010) The quinone-binding sites of the cytochrome bo_3 ubiquinol oxidase from *Escherichia coli*. *Biochim. Biophys. Acta 1797*, 1924–1932.

(23) Kita, K., Konishi, K., and Anraku, Y. (1984) Terminal oxidases of *Escherichia coli* aerobic respiratory chain. *J. Biol. Chem. 259*, 3368–3374.

(24) Sena, F. V., Batista, A. P., Catarino, T., Brito, J. A., Archer, M., Viertler, M., Madl, T., Cabrita, E. J., and Pereira, M. M. (2015) Type-II NADH:quinone oxidoreductase from *Staphylococcus aureus* has two distinct binding sites and is rate limited by quinone reduction. *Mol. Microbiol. 98*, 272−288.

(25) Hazan, R., Que, Y. A., Maura, D., Strobel, B., Majcherczyk, P. A., Hopper, L. R., Wilbur, D. J., Hreha, T. N., Barquera, B., and Rahme, L. G. (2016) Auto poisoning of the respiratory chain by a quorum-sensing-regulated molecule favors biofilm formation and antibiotic tolerance. *Curr. Biol. 26*, 1−12.

(26) Filkins, L. M., Graber, J. A., Olson, D. G., Dolben, E. L., Lynd, L. R., Bhuju, S., and O'Toole, G. A. (2015) Coculture of *Staphylococcus aureus* with *Pseudomonas aeruginosa* drives *S. aureus* towards fermentative metabolism and reduced viability in a cystic fibrosis model. *J. Bacteriol. 197*, 2252–2264.

(27) Müller, C., Birmes, F. S., Niewerth, H., Fetzner, S. (2014) Conversion of the *Pseudomonas aeruginosa* quinolone signal (PQS) and related alkylhydroxyquinolines by *Rhodococcus* sp. strain BG43. *Appl. Environ. Microbiol. 80*, 7266–7274.

(28) Zhang, S., Chen, G., Chu, J., Wu, B., and He, B. (2014) High production of succinyl isoflavone glycosides by *Bacillus licheniformis* ZSP01 resting cells in aqueous miscible organic medium. *Biotechnol. Appl. Biochem. 62*, 255−259.

(29) Pandey, R. P., Li, T. F., Kim, E. H., Yamaguchi, T., Park, Y. I., Kim, J. S., and Sohng, J. K. (2013) Enzymatic synthesis of novel phloretin glucosides. *Appl. Environ. Microbiol. 79*, 3516−3521.

(30) Pandey, R. P., Gurung, R. B., Parajuli, P., Koirala, N., Tuoi, L. T., and Sohng, J. K. (2014) Assessing acceptor substrate promiscuity of YjiC-mediated glycosylation toward flavonoids. *Carbohydr. Res. 393*, 26−31.

(31) Parajuli, P., Pandey, R. P., Koirala, N., Yoon, Y. J., and Sohng, J. K. (2014) Enzymatic synthesis of epothilone A glycosides. *AMB Express 4*, 31.

(32) Parajuli, P., Pandey, R. P., Pokhrel, A. R., Ghimire, G. P., and Sohng, J. K. (2014) Enzymatic glycosylation of the topical antibiotic mupirocin. *Glycoconj. J. 31*, 563−572.

(33) Häggblom, M. M., Nohynek, L. J., and Salkinoja-Salonen, M. S. (1988) Degradation and *O*-methylation of chlorinated phenolic compounds by *Rhodococcus* and *Mycobacterium* strains. *Appl. Environ. Microbiol. 54*, 3043–3052.

(34) Kim, Y.-H., Moody, J. D., Freeman, J. P., Brezna, B., Engesser, K.-H., and Cerniglia, C. E. (2004) Evidence for the existence of PAH-quinone reductase and catechol-*O*-methyltransferase in *Mycobacterium vanbaalenii* PYR-1. *J. Ind. Microbiol. Biotechnol. 31*, 507–516.

(35) Nappi, A. J., and Vass, E. (1998) Hydroxyl radical formation via iron-mediated Fenton chemistry is inhibited by methylated catechols. *Biochim. Biophys. Acta 1425*, 159–167.

(36) Lamprecht, D. A., Finin, P. M., Rahman, A., Cumming, B. M., Russell, S. L., Jonnala, S. R., Adamson, J. H., and Steyn, A. J. C. (2016) Turning the respiratory flexibility of *Mycobacterium tuberculosis* against itself. *Nat. Commun. 7*, 1–14.

(37) Lightbown, J. W., and Jackson, F. L. (1956) Inhibition of cytochrome systems of heart muscle and certain bacteria by the antagonists of dihydrostreptomycin: 2-alkyl-4-hydroxyquinoline *N*-oxides. *Biochem. J. 63*, 130−137.

(38) Machan, Z. A., Taylor, G. W., Pitt, T. L., Cole, P. J., and Wilson, R. (1992) 2-Heptyl-4-hydroxyquinoline *N*-oxide, an antistaphylococcal agent produced by *Pseudomonas aeruginosa. J. Antimicrob. Chemother. 30*, 615−623.

(39) Lanciano, P., Khalfaoui-Hassani, B., Selamoglu, N., Ghelli, A., Rugolo, M., and Daldal, F. (2013) Molecular mechanisms of superoxide production by complex III: a bacterial versus human mitochondrial comparative case study. *Biochim. Biophys. Acta 1827*, 1332−1339.

(40) Chen, X., Zhong, Z., Xu, Z., Chen, L., and Wang, Y. (2010) 2′,7′-Dichlorodihydrofluorescein as a fluorescent probe for reactive oxygen species measurement: Forty years of application and controversy. *Free Radic. Res. 44*, 587–604.

(41) Matsoso, L. G., Kana, B. D., Crellin, P. K., Lea-Smith, D. J., Pelosi, A., Powell, D., Dawes, S. S., Rubin, H., Coppel, R. L., and Mizrahi, V. (2005) Function of the cytochrome bc_1-aa_3 branch of the respiratory network in mycobacteria and network adaptation occurring in response to its disruption. *J. Bacteriol. 187*, 6300–6308.

(42) Winstedt, L., and von Wachenfeldt, C. (2000) Terminal oxidases of *Bacillus subtilis* strain 168: one quinol oxidase, cytochrome aa_3 or cytochrome *bd*, is required for aerobic growth. *J. Bacteriol. 182*, 6557–6564.

(43) Borisov, V. B., Gennis, R. B., Hemp, J., and Verkhovsky, M. I. (2011) The cytochrome *bd* respiratory oxygen reductases. *Biochim. Biophys. Acta 1807*, 1398–1413.

(44) Lemma, E., Simon, J., Schagger, H., and Kröger, A. (1995) Properties of the menaquinol oxidase (Qox) and of *qox* deletion mutants of *Bacillus subtilis*. *Arch. Microbiol. 163*, 432–438.

(45) Hammer, N. D., Schurig-Briccio, L. A., Gerdes, S. Y., Gennis, R. B., and Skaar, E. P. (2016) CtaM is required for menaquinol oxidase aa_3 function in *Staphylococcus aureus*. *MBio 7*, e00823–16.

(46) Voggu, L., Schlag, S., Biswas, R., Rosenstein, R., Rausch, C., and Götz, F. (2006) Microevolution of cytochrome *bd* oxidase in staphylococci and its implication in resistance to respiratory toxins released by *Pseudomonas*. *J. Bacteriol. 188*, 8079–8086.

(47) Rampioni, G., Falcone, M., Heeb, S., Frangipani, E., Fletcher, M. P., Dubern, J.-F., Visca, P., Leoni, L., Cámara, M., and Williams, P. (2016) Unravelling the genome-wide contributions of specific 2-alkyl-4-quinolones and PqsE to quorum sensing in *Pseudomonas aeruginosa*. PLoS Pathog. *12(11)*: e1006029.

(48) Reen, F. J., Clarke, S. L., Legendre, C., McSweeney, C. M., Eccles, K. S., Lawrence, S. E., O'Gara, F., and McGlacken, G. P. (2012) Structure–function analysis of the C-3 position in analogues of microbial behavioural modulators HHQ and PQS. *Org. Biomol. Chem. 10*, 8903–8910.

(49) Woschek, A., Mahout, M., Mereiter, K., and Hammerschmidt, F. (2007) Synthesis of 2-heptyl-1-hydroxy-4(1H)-quinolone – unexpected rearrangement of 4-(alkoxycarbonyloxy)quinoline *N*-oxides to 1-(alkoxycarbonyloxy)-4(1*H*)-quinolones. *Synthesis 10*, 1517–1522.

(50) Diep, B. A., Gill, S. R., Chang, R. F., Phan, T. H., Chen, J. H., Davidson, M. G., Lon, F., Lin, J., Carleton, H. A., Mongodin, E. F., Sensabaugh, G. F., and Perdreau-Remington, F. (2006) Complete genome sequence of USA300, an epidemic clone of community-acquired methicillin-resistant *Staphylcoccus aureus*. *The Lancet 367*, 731−739.

524

FIGURE LEGENDS

Figure 1. Biotransformation of HQNO by cell suspensions (initial $OD_{600\ nm}$ of 2.0) of *B. subtilis* 168, *M. abscessus* DSM 44196, and *S. aureus* Newman. Conversion of HQNO (black squares) led to transient formation of: (a) G-HQNO (blue filled squares) and SG-HQNO (blue open squares) by *B. subtilis* 168; (b) HMOQ (red squares) by *M. abscessus* DSM 44196; (c) PQS-NO (green squares) by *S. aureus* Newman. Symbols and error bars represent the means and standard errors of three biological replicates. Culture media or spent media did not mediate conversion of HQNO.

Figure 2. Inhibitory effect of HQNO and key metabolites on cellular respiration and menaquinol oxidase. The effect of HQNO (black), G-HQNO (blue), HMOQ (red), and PQS-NO (green) on oxygen consumption by cell suspensions is shown in (a, b, c), while effects on the menaquinol oxidase activity of membrane fractions are shown in (d, e, f). Panels (a, d): *B. subtilis* 168; (b, e): *M. abscessus* DSM 44196; (c, f): *S. aureus* Newman. Data were normalized to cellular/enzymatic O_2 consumption rates (cOCR/eOCR) of the respective reference measurement (without inhibitor) which was set to 100 %. Symbols and error bars represent the means and standard errors of three biological replicates. EC_{50} values (see text) were estimated by fitting the data to dose response curves (solid lines).

Figure 3. Relative increase of the fluorescence intensity of DCF, a probe for cellular ROS, in the presence of HQNO and key metabolites. H_2DCF-DA treated cells of *B. subtilis* 168, *M. abscessus* DSM 44196 and *S. aureus* Newman were incubated for 30 min with 100 µM of HQNO (dark bars), and 100 µM of G-HQNO (blue bar), HMOQ (red bar), and PQS-NO (green bar),

respectively. Each bar, which is normalized to the fluorescence increase of the respective control containing only DMSO, and error bar represent the mean ± SE of three independent experiments, each measured in three technical replicates. One-way ANOVA was used for statistical analysis, * $P<0.02$, ** $P<0.01$ and *** $P<0.0001$.

Figure 4. Overview of the effects of HQNO and its metabolites on the respective bacterial species. Inhibition of quinol oxidase activity, as indicated by EC_{50} values, is reduced by HQNO conversion. Metabolites in comparison to HQNO induced less cellular oxidant stress, as indicated by fold changes in cellular ROS production (ROS levels in DMSO controls set to 1).

TABLE

Table 1. Key metabolites of HQNO conversion.

Organisms	**HQNO Metabolites**			
	RT [a]	***m/z* [M + H^+]** [b]	**Fragment Ions** [b]	**Structure** [c]
B. subtilis [d] *B. licheniformis*	13.9 min	422.217	260.16391	G-HQNO 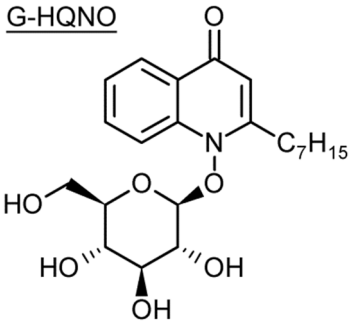
M. abscessus [d] *M. fortuitum* *M. smegmatis*	25.2 min	274.1801	159.06853 186.09225 172.076511	HMOQ 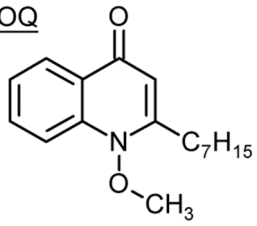
S. aureus *R. erythropolis* *A.* sp. Rue61a [d] *P. aurescens*	23.5 min	276.159	175.06265 178.04974 188.07055	PQS-NO 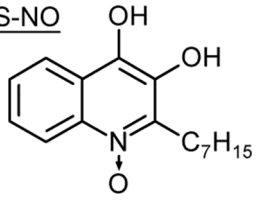

[a] HPLC retention time.

[b] MS and MS/MS data of the key metabolites. See also Supporting Information, Figure S1-S3.

[c] Structure proposal based on MS and NMR data. See also Supporting Information, Figure S4-S6.

[d] denotes the organism cultivated for preparative isolation of the respective metabolite.

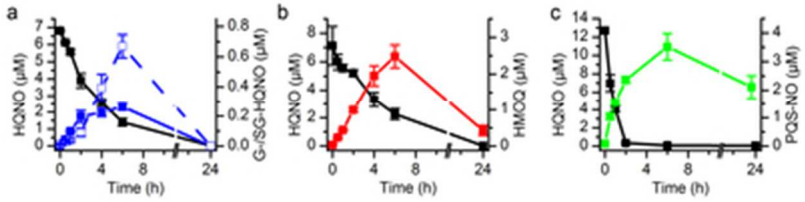

Figure 1. Biotransformation of HQNO by cell suspensions (initial OD600 nm of 2.0) of B. subtilis 168, M. abscessus DSM 44196, and S. aureus Newman. Conversion of HQNO (black squares) led to transient formation of: (a) G-HQNO (blue filled squares) and SG-HQNO (blue open squares) by B. subtilis 168; (b) HMOQ (red squares) by M. abscessus DSM 44196; (c) PQS-NO (green squares) by S. aureus Newman. Symbols and error bars represent the means and standard errors of three biological replicates. Culture media or spent media did not mediate conversion of HQNO.

34x8mm (300 x 300 DPI)

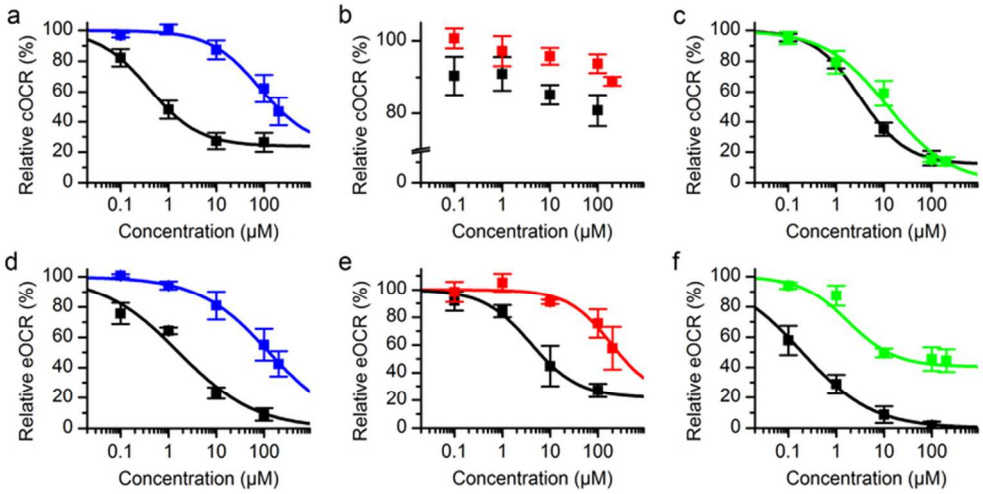

Figure 2. Inhibitory effect of HQNO and key metabolites on cellular respiration and menaquinol oxidase. The effect of HQNO (black), G-HQNO (blue), HMOQ (red), and PQS-NO (green) on oxygen consumption by cell suspensions is shown in (a, b, c), while effects on the menaquinol oxidase activity of membrane fractions are shown in (d, e, f). Panels (a, d): B. subtilis 168; (b, e): M. abscessus DSM 44196; (c, f): S. aureus Newman. Data were normalized to cellular/enzymatic O2 consumption rates (cOCR/eOCR) of the respective reference measurement (without inhibitor) which was set to 100 %. Symbols and error bars represent the means and standard errors of three biological replicates. EC50 values (see text) were estimated by fitting the data to dose response curves (solid lines).

69x34mm (300 x 300 DPI)

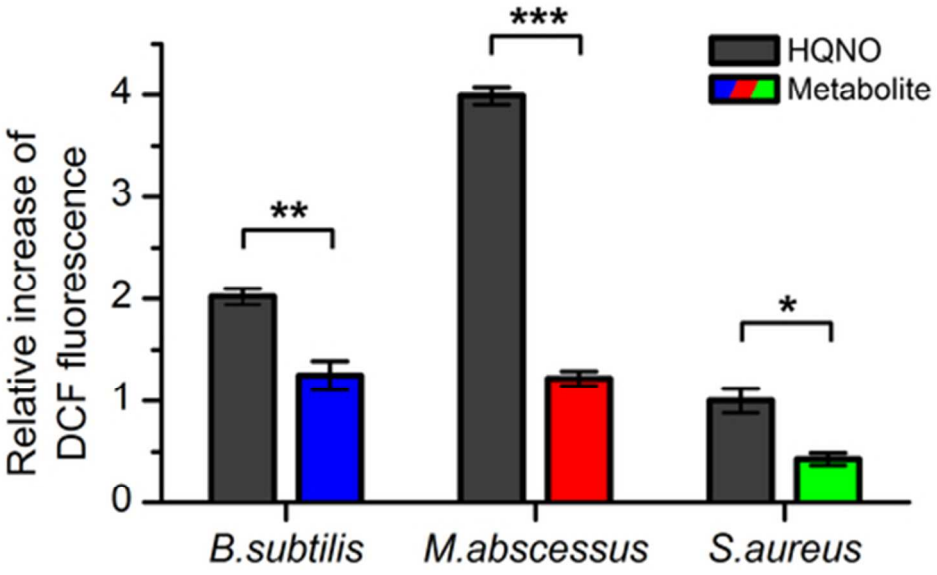

Figure 3. Relative increase of the fluorescence intensity of DCF, a probe for cellular ROS, in the presence of HQNO and key metabolites. H2DCF-DA treated cells of B. subtilis 168, M. abscessus DSM 44196 and S. aureus Newman were incubated for 30 min with 100 μM of HQNO (dark bars), and 100 μM of G-HQNO (blue bar), HMOQ (red bar), and PQS-NO (green bar), respectively. Each bar, which is normalized to the fluorescence increase of the respective control containing only DMSO, and error bar represent the mean ± SE of three independent experiments, each measured in three technical replicates. One-way ANOVA was used for statistical analysis, * P<0.02, ** P<0.01 and ***P<0.0001.

40x25mm (300 x 300 DPI)

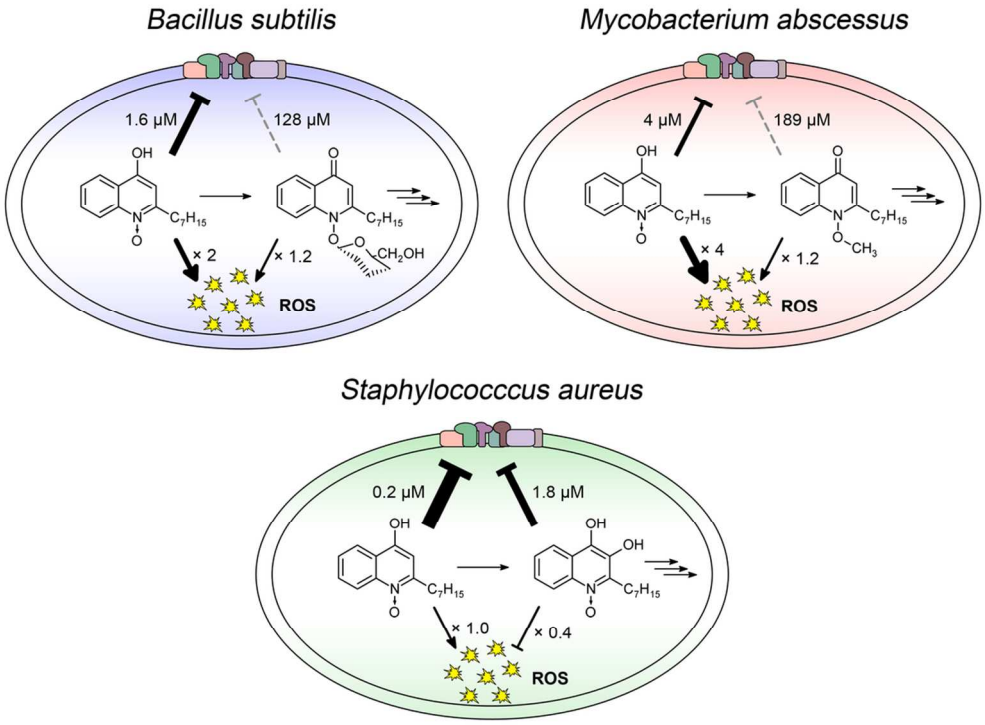

Figure 4. Overview of the effects of HQNO and its metabolites on the respective bacterial species. Inhibition of quinol oxidase activity, as indicated by EC50 values, is reduced by HQNO conversion. Metabolites in comparison to HQNO induced less cellular oxidant stress, as indicated by fold changes in cellular ROS production (ROS levels in DMSO controls set to 1).

102x75mm (300 x 300 DPI)

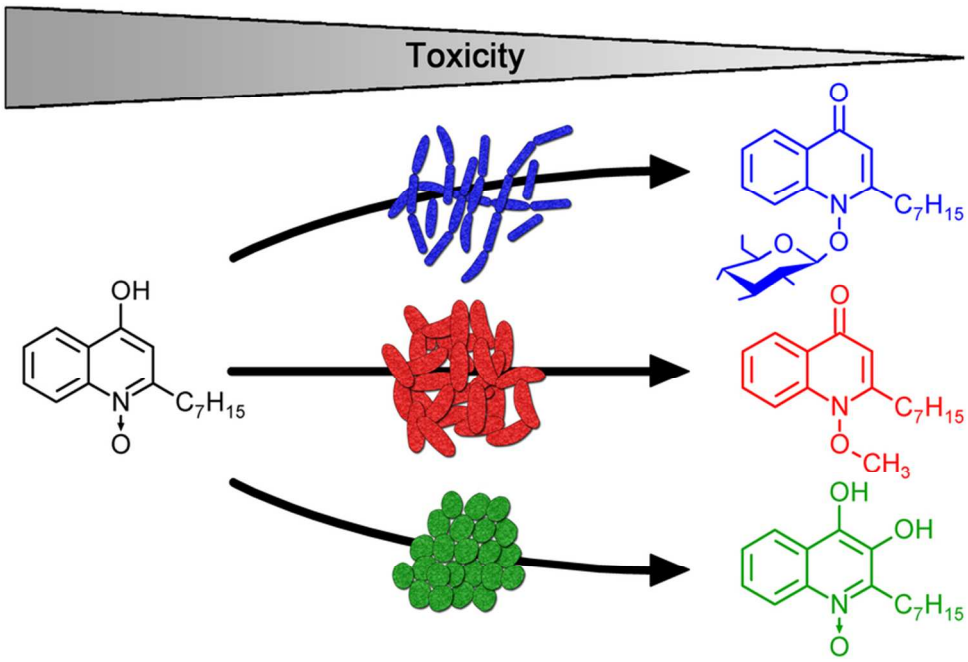

TOC graph

40x26mm (600 x 600 DPI)